

# Electromagnetic scattering from complex conjugate cylinder of infinite length

A. ILLAHI<sup>a</sup>, M. BASHIR<sup>c</sup>, P. IFTIKHAR<sup>a</sup>, Q. A. NAQVI<sup>c</sup>, A. GHUFFAR<sup>d</sup>, M. Y. NAZ<sup>b</sup>, A. GHAFFAR<sup>b,\*</sup>

<sup>a</sup>RIMS Group, Department of Physics, COMSATS University, Islamabad, Pakistan

<sup>b</sup>Department of Physics, University of Agriculture, Faisalabad, Pakistan

<sup>c</sup>Department of Electronics, Quaid-i-Azam University, Islamabad, Pakistan

<sup>d</sup>Department of Physics, Riphah International University Faisalabad Campus, Faisalabad, Pakistan

<sup>e</sup>Department of Electrical Engineerings, University of Management and Technology, Lahore, Pakistan

A plane wave interacts with a complex conjugate medium (CCM) circular cylinder of radius  $a$ . The cylinder is placed in free space. Taking in account the classical scattering theory, the incident and scattered fields are found. By solving the boundary value problem, the unknown coefficients and scattered fields are formulated. Numerical results are found by plotting the echo width, scattered and transmitted fields with size parameter of the cylinder, observation angle and imaginary part of the refractive index. Comparison of obtained numerical results for limiting cases is done with published literature and has been found in good agreement. It has been shown that the scattering from CCM cylindrical geometry is larger than standard dielectric. Both the TE and TM polarizations of incident plane wave have been used in the analysis.

(Received August 11, 2018; accepted June 14, 2019)

**Keywords:** Scattering, Complex conjugate medium, Optical properties

## 1. Introduction

It is well known that the electrons are tightly bound in non-conducting materials. They are not readily available for the conduction. The negative electron cloud is whirling around the positive nucleus. There is a very symmetrical pattern before applying the electromagnetic wave. The material becomes distorted when the electric field is applied. The positive and negative charges are displaced. So, the electric phenomenon is stored in the resulting configuration. This response is denoted by the permittivity of the material. Similarly, when the magnetic field is applied, the magnetic poles become twisted. Hence the magnetic phenomenon can be stored in this way. This response of the material is called the permeability of the material. Permittivity and permeability of the material are in general complex [1]. But if the choice is made in such a way that the imaginary part of the relative permittivity ( $\epsilon_r$ ) and relative permeability ( $\mu_r$ ) is cancelled out in the refractive index ( $n$ ) i.e.,  $\epsilon_r = m(a - ib)$  and  $\mu_r = a + ib$  and hence  $n = \sqrt{m(a^2 + b^2)}$ , where  $a$  and  $b$  are real parameters and  $m$  is any positive constant. Then that material is called complex conjugate material (CCM) [2]. CCM is electrically active and magnetically dissipative here according to the assumed time dependency  $e^{j\omega t}$  and can be other way round depending on the sign of  $b$ . The gain coefficient in optical active materials (e.g. in the non-impurified non-magnetic semiconductor nano-sized lasers) is controlled by injection current. It can be tuned to the value required by CCM when Mn is used as dopant. Thus, CCM can be realized using the existing technology [2].

Over the past several decades, a significant amount of research struggle has been spent towards developing the scattering theory. The detectability of the obstacle always

had an immense importance in different fields of science e.g. medical science, defense purposes, under water detection of the obstacles for different requirements, buried objects detection and so on. Scattering theory is a very key tool of physics. It provides many important evidences about the particles or obstacles [3].

Out of many problems in scattering theory, scattering of electromagnetic waves by circular cylinder has gained the attention of the investigators [12], reason why the cylinders got so much importance in scientific research was the geometrical symmetry and various objects in daily life were of cylindrical shape e.g. human body, buildings, aero planes, submarines and pipes which can be modelled by the cylinder. Interaction of electromagnetic waves and different antennas in the close vicinity of cylinders enhances the directivity of antennas. Furthermore, most of the antennas are in cylindrical shape. In order to get valuable findings from these practical geometries regarding interaction of electromagnetic waves cylinder can be utilized [4-12].

In this paper electromagnetic interaction with the cylindrical geometry made up of CCM is considered. In case of cylindrical geometry, two cases of plane wave incidence have been considered, i.e.,  $TM^z$  and  $TE^z$ .

In case of  $TM^z$  wave incidence, electric field is taken as parallel to the cylinder axis and the magnetic field is perpendicular to the direction of wave propagation. In case of  $TE^z$  wave incidence, magnetic field is taken as parallel to the cylinder axis and the electric field is perpendicular to the direction of wave propagation.

## 2. Formulation of problem

Consider a circular cylinder of CCM, whose relative permittivity and relative permeability both are scalar and

satisfy the complex conjugate material condition i.e.  $\epsilon_r = m\mu_r^*$ , where  $\mu_r^*$  is the complex conjugate of  $\mu_r$  and  $m$  is any positive constant [2]. Let the axis of the cylinder is to be parallel to the  $z$ -axis as shown in Fig. 1.

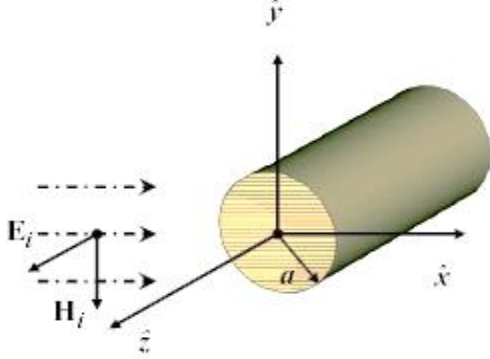


Fig. 1. Geometry of cylinder in case of TM incident wave

Let us assume that an incident plane wave having TM<sup>z</sup> polarization with the H-field perpendicular to axis of the cylinder contains the incident propagation vector  $k$  in the  $x$ -direction as follows.

$$\mathbf{E}^i = \hat{\mathbf{z}}E_0 e^{jk\rho\cos\phi}$$

The direction of wave propagation is taken along  $x$  axis. As the target geometry is cylinder, therefore it was necessary to transform the plane wave into sum of cylindrical wave functions which are of course Bessel  $J_n(\cdot)$  and Hankel functions  $H_n^{(k)}(\cdot)$ .

$$E_z^i = E_0 \sum_{n=-\infty}^{\infty} j^{-n} J_n(k_0\rho) e^{jn\phi} \quad (1)$$

The scattered field can be assumed to have the following form of Eq. (2). As the time dependency of the wave is assumed to be positive ( $e^{j\omega t}$ ) therefore Hankel function of the first kind represents the wave travelling towards the cylinder whereas Hankel function of the second kind represents the wave travelling away from the cylinder. Bessel function instead of Hankel function is used to avoid the singularity at the origin.

$$E_z^s = E_0 \sum_{n=-\infty}^{\infty} j^{-n} a_n H_n^{(2)}(k_0\rho) e^{jn\phi} \quad (2)$$

whereas the transmitted fields are:

$$E_z^t = E_0 \sum_{n=-\infty}^{\infty} j^{-n} b_n J_n(k_1\rho) e^{jn\phi} \quad (3)$$

Using Maxwell equations incident magnetic fields have been found. Scattered fields have been formulated on the same patterns as that of incident field but with unknown coefficients. Similarly, transmitted magnetic fields have been found, all with unknown coefficients. These unknown coefficients then have been found using the boundary conditions which have been found through the continuity of electric and magnetic fields. Now in order to calculate the

coefficients  $a_n$  and  $b_n$  we need only to calculate the tangential components of magnetic field ( $H$ ) i.e.  $H_\phi$  we can also do this for the scattered and transmitted field. These fields can be found immediately from Maxwell Equations. Then imposing the boundary conditions i.e.

$$E_z^i + E_z^s = E_z^t \quad (4)$$

$$H_\phi^i + H_\phi^s = H_\phi^t \quad (5)$$

where  $z$  and  $\phi$  denote the tangential components.

Substituting the expressions of  $E_z$  and  $H_\phi$  into the above equations we get

$$a_n = \frac{J_n(k_0 a) J_n(k_1 a) - \sqrt{\frac{\epsilon_r}{\mu_r}} J_n(k_0 a) J_n(k_1 a)}{\sqrt{\frac{\epsilon_r}{\mu_r}} J_n(k_1 a) H_n^{(2)}(k_0 a) - J_n(k_1 a) H_n^{(2)}(k_0 a)} \quad (6)$$

$$b_n = \frac{J_n(k_0 a) H_n^{(2)}(k_0 a) - J_n(k_0 a) H_n^{(2)}(k_0 a)}{J_n(k_1 a) H_n^{(2)}(k_0 a) - \sqrt{\frac{\epsilon_r}{\mu_r}} J_n(k_1 a) H_n^{(2)}(k_0 a)} \quad (7)$$

Computing for TE<sup>z</sup>-Polarization

$$a_n = \frac{J_n(k_0 a) J_n(k_1 a) - \sqrt{\frac{\mu_r}{\epsilon_r}} J_n(k_0 a) J_n(k_1 a)}{\sqrt{\frac{\mu_r}{\epsilon_r}} J_n(k_1 a) H_n^{(2)}(k_0 a) - J_n(k_1 a) H_n^{(2)}(k_0 a)} \quad (8)$$

$$b_n = \frac{J_n(k_0 a) H_n^{(2)}(k_0 a) - J_n(k_0 a) H_n^{(2)}(k_0 a)}{J_n(k_1 a) H_n^{(2)}(k_0 a) - \sqrt{\frac{\mu_r}{\epsilon_r}} J_n(k_1 a) H_n^{(2)}(k_0 a)} \quad (9)$$

Utilizing these unknown coefficients in the scattered and transmitted fields, they have been fixed. In order to find the fields at the far zones, asymptotic forms of Bessel and Hankel function have been used [12]. Then square of amplitudes of the incident and scattered fields has given us the intensities of the incident and scattered fields. These intensities then have been utilized in finding the echo width of the cylinder which is also the measure of apparent area of cross section of the cylinder. Echo width of the CCM cylinder is found and compared with the standard dielectric cylinder.

### 3. Radar cross section (echo-width)

Presence of cylinder and background field gives rise to the relative field which is the difference between the measured fields. It is then used to define the detect ability of radar, so the RCS of a 2D scatterer is explicitly elaborated as [12]

$$\sigma_{2D} = \lim_{\rho \rightarrow \infty} 2\pi\rho \frac{|E^s|^2}{|E^i|^2} \quad (10)$$

#### 4. Results and discussion

In this section numerical results have been presented. Two cases have been considered. In the first case, the numerical results for  $TM^Z$  polarization have been presented and in the second case the  $TE^Z$  polarization is discussed. The unknown coefficients are obtained and results have been discussed graphically.

##### 4.1. $TM^Z$ -Polarization

In  $TM^Z$  polarization case, electric field is taken as parallel to the axis of the cylinder (i.e. z-axis), whereas magnetic field is taken as transverse to the axis of the cylinder. In this case the direction of incident wave is taken as along x axis. The electric and magnetic fields directions are transformed in cylindrical coordinates. The scattered fields are calculated. The “far” fields are formulated using the asymptotic forms for large argument of Hankel and Bessel function. The radar cross section or echo width has been calculated using equation (10) and plotted against various parameters in Fig. 2 (a-d).

Fig. 2 (a) shows the comparison of echo width of CCM cylinder with the standard dielectric cylinder. Parameters for the standard dielectric material are taken as  $\epsilon_r = 4$ ,  $\mu_r = 1$  and  $ka = 4$ . The size parameter  $ka$  for CCM is also taken as 4. The relative permittivity and the permeability of the medium is  $4(1 - ib)$ ,  $1 + ib$ , respectively. The imaginary part of the permittivity and permeability is represented by  $b$ . In this case the value of  $b$  is taken as 3. This figure shows that the scattering in the case of complex conjugate medium is dominating over the standard dielectric material. This is due to the fact that imaginary part of the relative permittivity and relative permeability of the medium is responsible for the losses. As in case of CCM this imaginary part is cancelled out and the medium becomes lossless. Hence it contributes to scattering instead of absorption. Hence the scattering dominates.

In Fig. 2 (b), we have compared our results with the standard dielectric material cylinder which are available in the literature [12]. The size parameter  $ka$  is taken as 4. The relative permittivity  $\epsilon_r$  and the permeability  $\mu_r$  of the medium is  $4(1 - ib)$ ,  $1 + ib$ , respectively. Here the value of  $b$  is zero. The parameters for the standard dielectric material are taken as  $\epsilon_r = 4$ ,  $\mu_r = 1$  and  $ka = 4$ . The result exactly matches with the published literature [12]. This also validated our formulation as well as our code.

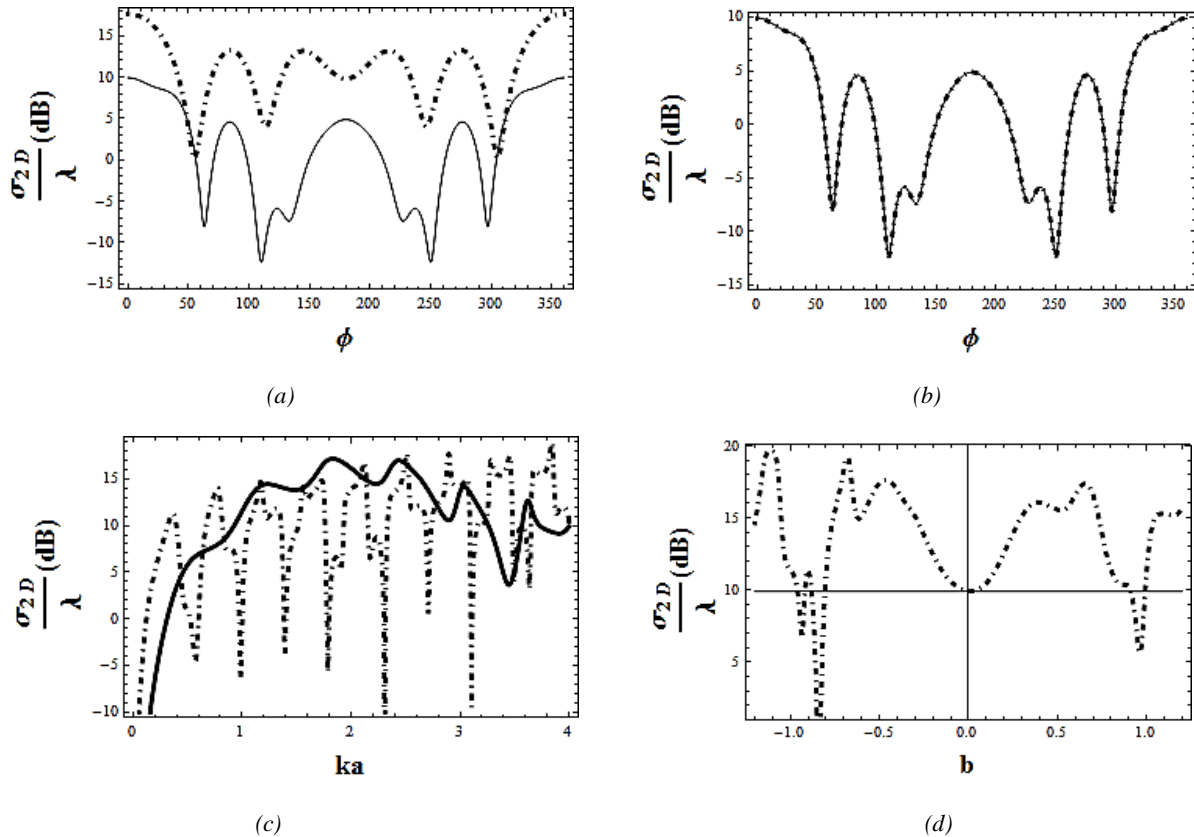


Fig. 2. (a) Normalized echo width versus observation angle (Solid line represents standard dielectric whereas dotted line represents CCM), (b) Normalized echo width versus observation angle with imaginary part of permittivity and permeability zero, (c) Normalized echo width with size parameter, (d) Normalized echo width versus imaginary part of permittivity and permeability

Fig. 2 (c) shows the variation of echo width with the size parameter. The dips in the oscillations are not due to the attenuation factor as the refractive index is real in case of CCM. The drastic variations in the fields are due to the multiple bounces by the surface of the cylinder and resonances inside the cylinder. These also affect the fields outside the cylinder [12]

Fig. 2 (d) explains the variation of echo width with the imaginary part of permittivity and/or permeability. The graph is compared with the lossless dielectric. The size parameter  $ka$  is taken as 4. The relative permittivity  $\epsilon_r$  and the permeability  $\mu_r$  of the medium is  $4(1 - ib)$ ,  $1 + ib$ , respectively. Here the value of  $b$  is varied between -1.2 to 1.2. The parameters for the standard dielectric material are taken as  $\epsilon_r = 4$ ,  $\mu_r = 1$ . The graph indicates that when  $b = 0$ , CCM curve exactly matches with that of the standard dielectric [12]. Here the lossless dielectric is shown by a horizontal straight line as it has no variation with  $b$  i.e., the imaginary part. This is again the verification of our formulation as well as of our code.

#### 4.2. TE<sup>Z</sup>-Polarization

In TE<sup>Z</sup> polarization case, magnetic field is taken as parallel to the axis of the cylinder, therefore electric field is taken as transverse to the direction of wave propagation. In this case the direction of incident wave is taken as along x axis. The electric and magnetic fields directions are transformed in cylindrical coordinates. The scattered fields are calculated. The “far” fields are formulated using the asymptotic forms far large argument of Hankel and Bessel function. The radar cross section or echo width has been calculated using equation (10) and plotted against various parameters in Fig. 3 (a-d). Parameters for the standard dielectric material are taken as  $\epsilon_r = 4$ ,  $\mu_r = 1$  and  $ka = 4$ , whereas the size parameter  $ka$  for CCM is also taken as 4. The relative permittivity and the permeability of the medium is  $4(1 - ib)$ ,  $1 + ib$ , respectively. Fig. 3(a) shows the comparison of echo width of CCM cylinder with the standard dielectric cylinder. The imaginary part of the permittivity and permeability is taken as 3. This figure shows that the scattering in the case of complex conjugate medium is dominating over the standard dielectric material. In Fig. 3 (b), we have compared our results with the standard dielectric material cylinder which are available in the literature [12]. The size parameter  $ka$  is taken as 4 for both standard dielectric as well as CCM. The relative permittivity  $\epsilon_r$  and the permeability  $\mu_r$  of the medium is  $4(1 - ib)$ ,  $1 + ib$ , respectively. Here the value of  $b$  is zero. The parameters for the standard dielectric material are taken as  $\epsilon_r = 4$ ,  $\mu_r = 1$  and  $ka = 4$ . The result exactly matches with the published literature [12]. This also validated our formulation as well as our code. Fig. 3 (c) shows the variation of echo width with the size parameter. The more oscillations in the TE case is due to the creeping waves that travel around the cylinder [12]. Fig. 3 (d) explains the variation of echo width with the imaginary part of permittivity and/or permeability. The rest of the parameters are same as preceding except  $b$  which

varies from -1.2 to 1.2. When  $b = 0$ , CCM curve exactly converges to that of the standard dielectric which is shown by a horizontal straight line as it has no variation with  $b$  i.e., the imaginary part.

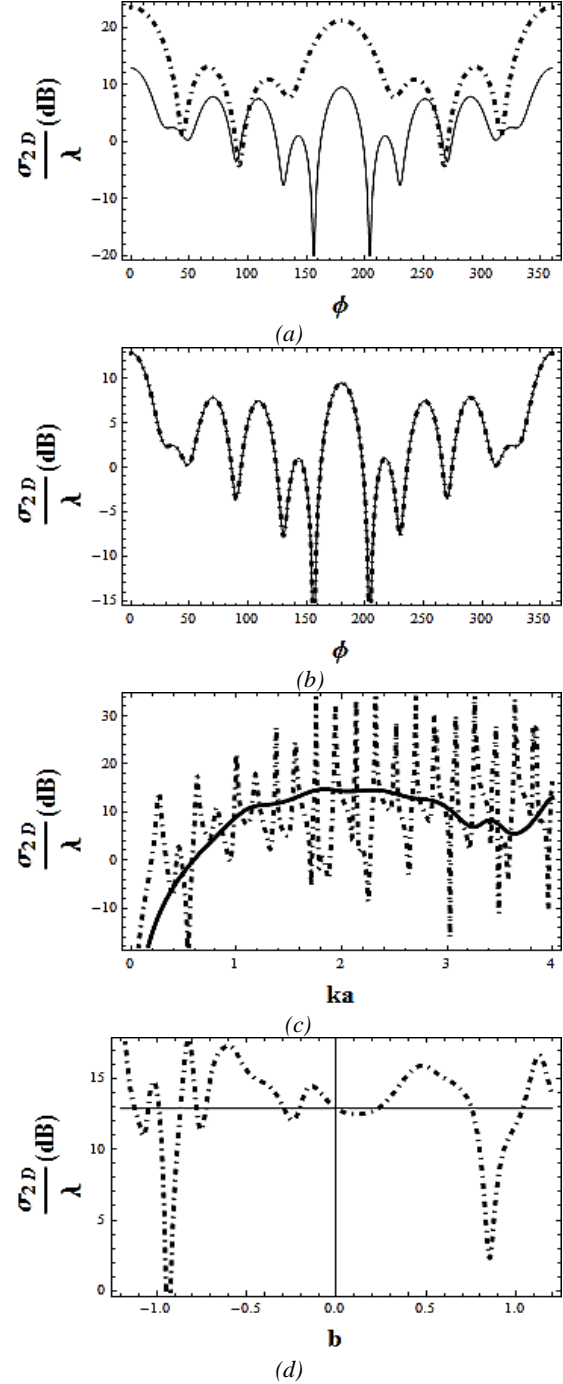


Fig. 3. (a) Normalized echo width versus observation angle (Solid line represents standard dielectric whereas dotted line represents CCM), (b) Normalized echo width versus observation angle with imaginary part of permittivity and permeability zero, (c) Normalized echo width with size parameter, (d) Normalized echo width versus imaginary part of permittivity and permeability

## 5. Conclusions

It has been shown that the scattering in the case of complex conjugate medium is dominating over the standard dielectric material. The reason is that the imaginary part of the relative permittivity and relative permeability of the medium is responsible for the losses. As in case of CCM this imaginary part is cancelled out in the expression of refractive index and the medium becomes lossless. Hence it contributes to scattering instead of absorption. Hence the scattering dominates. Then we compared our results with the standard dielectric material cylinder which are available in the literature. The results exactly match with the published literature [12]. This also validated our formulation as well as our code. Furthermore, the variation of echo width with the imaginary part of permittivity and/or permeability is observed. The results are compared with the lossless dielectric. The results exactly match with that of the standard dielectric [12]. This is again the verification of our formulation as well as our code. It is concluded that the scattering in the case of CCM is dominant over the standard dielectric. So, the coating with CCM may find potential application in the detection.

## Acknowledgements

Authors would like to acknowledge the useful comments of Prof. Raymond Rumpf, University of Texas at El Paso during this work.

## References

- [1] D. J. Griffiths, *Introduction to Electrodynamics*, Cambridge University Press, 2017.
- [2] D. Dragoman, *Optics Communications* **284**, 2095 (2011).
- [3] H. C. van de Hulst, *Light Scattering by Small Particles*, Courier Corporation, 2012.
- [4] Yao, Hai-Ying, Le-Wei Li, Cheng-Wei Qiu, Qun Wu, Zhi-Ning Chen, *Radio Science* **42**(RS2006), 2007.
- [5] D. Das, *Journal of Ocean Engineering and Science* **1**, 135 (2016).
- [6] A. Lakhtakia, J. B. Geddes III, *AEU-International Journal of Electronics and Communications* **61**, 62 (2007).
- [7] K. Hongo, *Antennas and Propagation, IEEE Transactions* **26**, 748 (1978).
- [8] A. Illahi, A. Ghaffar, I. Shakir, M. M. Ali, K. M. Ahmed, M. Naveed, Q. A. Naqvi, *Optik* **127**, 11143 (2016).
- [9] S. Iqbal, M. Fiaz, M. Ashraf, *AEU-International Journal of Electronics and Communications* **70**, 58 (2016).
- [10] A. Illahi, Q. A. Naqvi, *Central European Journal of Physics* **7**(4), 829 (2009).
- [11] A. Illahi, M. Afzaal, Q. A. Naqvi, *Progress In Electromagnetics research Letters* **4**, 43 (2008).
- [12] Jin Jian-Ming, *Theory and Computation of Electromagnetic Fields*, Wiley, 2015.

\*Corresponding author: chabdulghaffar@yahoo.com